EUROPEAN ORGANIZATION FOR NUCLEAR RESEARCH

Paper submitted to the
XIVth International Conference
on High-Energy Physics,
Vienna, 28 August - 5 September 1968

OBSERVATION OF THE RARE DECAY MODE OF THE φ MESON: $\varphi \rightarrow e^+e^-$

D. Bollini, A. Buhler-Broglin, P. Dalpiaz, T. Massam, F. Navach,
F.L. Navarria, M.A. Schneegans and A. Zichichi

CERN, Geneva, Switzerland.

Istituto di Fisica dell'Università di Bologna, Italy.

Istituto Nazionale di Fisica Nucleare, Sezione di Bologna, Italy.

Centre de Recherches Nucléaires, Strasbourg, France.

Geneva - 31 May 1968

SIS/K 0 784

"OBSERVATION OF THE RARE DECAY MODE OF THE φ MESON: $\varphi \to e^+e^-$"

1. INTRODUCTION AND PRINCIPLE OF THE METHOD

We report here the results of an experiment designed to detect the decay mode:

$$\varphi \to e^+ + e^- . \qquad (1)$$

The φ mesons were produced, at 1.93 GeV/c incident pion momentum in the reaction:

$$\pi^- + p \to n + V^o \quad (V^o \to e^+ + e^-) , \qquad (2)$$

where V^o stands for any neutral state.

The mass of the neutral state V^o was determined to ±15 MeV by simultaneous measurements of the velocity and direction of the neutron.

The decay of the neutral state V^o into an electron-positron pair was identified by means of two large electron detectors, similar to those originally designed by us[1] in order to achieve a high rejection power against pions. The knowledge of the e^+e^- energies and of their opening angle allowed a second determination of the V^o mass, and an increase in the rejection against spurious events. The weighted mean of the two mass values was used in the analysis.

2. EXPERIMENTAL SET-UP

Figure 1 shows a sketch of the experimental set-up, consisting of a beam telescope, a liquid hydrogen target, two electron detectors, and two neutron counters. The electron detectors "TOP" and "BOTTOM" were placed at 36° above and below the beam line, respectively. The neutron counters "RIGHT" and "LEFT" were set at an angle of 26° to the right and to the left of the beam.

The electron detectors were mounted on a turn-table and the neutron counters on rails for easy displacement into the direct beam for calibration.

2.1 The beam telescope

The beam was defined by counters U, S, and $\bar{R}$. U gave the zero time reference for the neutron time-of-flight, and was designed to handle high rates without loss of precision in the time measurements. Č was a threshold gas Čerenkov counter used to select pions or electrons for calibration purposes, and to reject electrons during the data-taking. $\bar{Q}$ vetoed non-interacting particles of the beam.

The liquid-hydrogen target was 40 cm long and 5 cm diameter, mounted at the centre of the turn-table which supported the two electron detectors.

2.2 The electron detectors

The electron detectors were identical, and therefore we will describe only one of them: TOP.

This detector consisted of:

i) a counter M_T to require incident charged particles and exclude high multiplicity: the efficiency was 92% for single particles, and negligible for three or more particles. This counter was made of three segments M_{T1}, M_{T2}, and M_{T3}, their signals being added linearly for pulse-height selection.

ii) Two six-gap thin-plate spark chambers, K_T, placed after M_T to record the incident particle direction and allow geometrical reconstruction with an accuracy of 1° in the electron direction.

iii) An electromagnetic shower detector with a powerful discrimination against pions. It consisted of a nine-layer sandwich of lead plates, optical spark chambers, and scintillators. The first lead plate of the sandwich was two radiation lengths thick in order to have a high probability of starting a shower, thus giving a high pulse-height in the first scintillator T_1. The other eight lead plates were each one radiation-length thick. The selection of electrons was made by simultaneous pulse-height discrimination on T_1 and on the sum Σ_T of the pulses from all nine scintillators. The best compromise between high pion rejection and high electron efficiency was obtained with the discrimination level on T_1 set at 1.7 times the mean pulse-height of minimum ionizing particles, and that on Σ_T set equal to the mean pulse-height expected for a 150 MeV electron. Under these conditions, the electronic efficiency for electron detection was 80% at 450 MeV/c and 94% at 1050 MeV/c. The corresponding pion rejection factors were 0.05 and 0.15.

A further rejection was achieved by spark counting and by a study of the collinearity between the incoming track and the axis of the shower.

In order to evaluate the mean electronic efficiency and study edge effects, the pulse-height distribution, electronic efficiency, and the number of sparks in the sandwich were measured for both pions and electrons as a function of their energy and of their position in the detector.

The over-all (electronic · visual) rejection against pions was 9×10^{-4} at 450 MeV/c and 6×10^{-4} at 1050 MeV/c, whilst the efficiencies for electron detection were 72% and 85%, respectively. Thus for coincidences between the two electron detectors, this gives an over-all rejection against hadronic decay modes of 5×10^{-7}.

2.3 The neutron detectors

Each neutron detector was constructed of two stacks of plastic scintillators placed one behind the other; each stack consisted of six counters, $18 \times 18 \times 100$ cm^3, with the long edge horizontal and orthogonal to the incident neutron direction.

Charged particles incident on the neutron detector were vetoed by the plastic scintillation counters G.

The time-of-flight and position measurements in a given counter were made using XP-104C photomultipliers coupled to the two 18×18 cm^2 faces. The dynode signals entered discriminators set to accept recoil proton energies greater than 18 MeV, and the outputs were used to gate the shaped anode signals which carried the timing information. The anode signals were shaped by discriminators set at a level 25% of the minimum pulse-height selected at the dynodes.

All the pulse heights of the neutron counters were equalized in the direct pion beam. Moreover, the counters were equalized in time to ±0.2 nsec, and were scanned across the beam to determine the calibration for the position measurement of the neutron. The calibration of the time-of-flight measurements was made using a calibrated delay box.

The uncertainty in locating the neutron interaction point in the detector was ±0.35° in polar angle and ±3° in azimuthal angle*). The electronic uncertainty in the time-of-flight was ±0.35 nsec. The mass resolution averaged over the experimental acceptance and including all uncertainties was ±15 MeV.

3. ELECTRONIC LOGIC (Fig. 2)

The incident beam was monitored by the coincidence $US\bar{R}$, whilst the coincidence $US\bar{R}\bar{C}\bar{Q} \equiv \overline{BEAM}$ recorded pions interacting in the target. A coincidence between $\overline{BEAM}$ and the first two counters T_1 and B_1 of the electron detectors provided a low rate signal which was used to gate the fast timing signal from counter U. This gated signal, called U_{time}, was used as the start-pulse in two time-to-analogue converters.

---

*) The azimuthal uncertainty is due to the vertical dimension of each neutron counter.

Since all the neutron counters were set at the same angle, the timing signals from corresponding ends of the detectors could be mixed without loss of information on the neutron velocity or scattering angle. These mixed signals are labelled 'side 1' and 'side 2' in Fig. 2, (cf. Fig. 1), and were used as the stop signals to give the neutron times-of-flight t_1 and t_2 observed by the photomultipliers at side 1 and side 2 of the neutron counters. They were also used to produce a third analogue signal proportional to the position P_ϑ of the neutron interaction point so that the neutron scattering angle ϑ could be calculated.

The signals P_ϑ and t_1 were then used in a fast matrix coincidence logic to define time-of-flight and angular limits for the neutron, so as to exclude high background regions in the $\vartheta - t_1$ scatter diagram (Fig. 3). An accepted neutron was denoted by the signal MASS.

The electronics of the two electron detectors were similar, so again we will describe only TOP: a coincidence, called e_T, between T_1, M_T, Σ_T, and $\overline{\text{BEAM}}$ indicated that a single charged particle had generated a shower in the first layer of the detector. Furthermore, signals Σ_T and the corresponding Σ_B for BOTTOM were added to give $\Sigma\Sigma$, proportional to the total energy of the two electrons. In the trigger, $\Sigma\Sigma$ was required to be greater than the mean pulse-height expected for 750 MeV electromagnetic energy release.

Coincidence conditions (M_{T1}, M_{B1}) and (M_{T3}, M_{B3}) vetoed the LEFT and the RIGHT neutron detector, respectively, since such coincidences corresponded to events with both neutron and electron pair emitted on the same side of the beam.

The solid angle not occupied by the electron detectors was covered by veto counters, in order to exclude as far as possible all except two-body decays of the resonance.

To summarize, the coincidence between the signals MASS, e_T, e_B, and $\Sigma\Sigma$ corresponded to an incident pion interaction which gave:

i) a neutron with very roughly selected kinematics;
ii) a low multiplicity event;
iii) a shower with greater than 150 MeV energy, starting early in each of the electron detectors;
iv) a total electromagnetic energy release greater than 750 MeV.

The FINAL coincidence triggered the spark chambers, and transferred the encoded signals t_1, t_2, P_ϑ, M_T, M_B, Σ_T, Σ_B, $\Sigma\Sigma$, and the neutron counter pattern to magnetic tape.

4. BACKGROUND

The first source of background is the random superposition of a charged particle and a γ-ray shower so as to simulate an electron. This effect is estimated by measuring the distribution of the distances between the charged pion and the γ ray, when they are resolved, and then extrapolating to distances too small to be resolved. This background was found to be negligible.

The second source of background is the simulation of electrons by γ rays which convert in the walls of the target or in the M counters, the subsequent pairs not being resolved in the K chambers. Figure 4 shows how we can evaluate this background. Here, all events which appear to have an electron in one electron detector have been included. The second electron detector may then contain either an electron or a converted γ ray, which is identified by the distance between the pair in the K chamber. The distribution of these distances is shown in Fig. 4. The true events are then observed as a peak at zero distance superimposed on a 25% background of unresolved pairs.

5. RESULTS AND DISCUSSION

Figure 5 shows the mass distribution of the events contained in the zero distance peak of Fig. 4. Clearly, the background is very low and we estimate it to be one-tenth of the φ peak. Thus the number of observed $\varphi \to e^+e^-$ events is 9 ± 3. A picture of the first event found is shown in Fig. 6.

On the basis of these data, the decay of the φ meson into an electron-positron pair is clearly established.

To the lowest order in α (the fine structure constant), the decay $\varphi \to e^+e^-$ is mediated by a single photon and, therefore, our experimental result is a direct proof that the φ-quantum numbers are: $J^{PC} = 1^{--}$. Further, it shows that the φ meson cannot be a pure SU(3) singlet*).

The absolute value of the cross-section for the production of φ mesons which decay into an electron-positron pair, is found to be

$$\sigma(\pi^- + p \to n + \varphi \hookrightarrow e^+e^-) = (18.4 \pm 6.9) \times 10^{-33} \text{ cm}^2 . \qquad (3)$$

*) This conclusion is based on the assumption, so far accepted as being valid, that the electromagnetic current is a pure SU(3) octet, i.e. without singlet term.

σ is calculated from the rate of observed events in our solid angle using the known efficiencies of the counters, the known production angular distribution[2] of the φ, and using zero polarization*) of the φ mesons. Radiative corrections for reaction (3) have been estimated[3] and found to be negligible (not more than a few per cent).

Using the total cross-section for φ production in $\pi^- p$ interactions at the same primary pion momentum[2]**):

$$\sigma(\pi^- + p \to n + \varphi) = (30 \pm 6)\,\mu b$$

we get the following value for the branching ratio:

$$\frac{\Gamma(\varphi \to e^+e^-)}{\Gamma(\varphi \to \text{total})} = (6.1 \pm 2.6) \times 10^{-4} \,. \qquad (4)$$

Using the total φ width[5]: $\Gamma(\varphi \to \text{total}) = (3.4 \pm 0.8)$ MeV, it is possible by means of Eq. (4), to derive the partial φ width:

$$\Gamma(\varphi \to e^+e^-) = (2.1 \pm 0.9) \text{ keV} \,. \qquad (5)$$

Theoretical predictions for this width have been obtained using different models[6-10], including the quark model[11]; a comparison with the experimental result [Eq. (5)] is shown in Table 1. Notice that all these models assume a large ω-φ mixing, and the range of predictions from 0.8 keV to 2.2 keV should be considered as an estimate of the theoretical uncertainty due to the various ways in which this large ω-φ mixing can be described.

---

*) The available data (Ref. 2) indicate that the φ has less than 20% polarization in our energy region. We can check this result, because we can calculate the angle ϑ_e between the electrons in the φ rest system and the normal to the φ-production plane. Our distribution of ϑ_e gives the maximum likelihood of zero polarization, well consistent with the above-mentioned data.

**) We have measured this cross-section at 2.1 GeV/c incident pion momentum, using only the neutron detector as neutral missing-mass spectrometer and two plastic scintillators to select predominantly the K^+K^- decay mode of the φ. Our value of $\sigma(\pi^- p \to n\,\varphi) = 21 \pm 7\,\mu b$ agrees very well with those obtained by Dahl et al[2], and by Boyd et al.[4].

Acknowledgements

We would like to express our thanks to Professors J.S. Bell, G. Cocconi, B.P. Gregory, P. Preiswerk and G. Puppi for their continuous support and interest.

We are very grateful to Mr. F. Blythe for the design of the electron detector support, to Mr. G. Pozzo for the realization of the neutron detector frame, and to Dr. L. Mazzone and Mr. C. Brand for the design of the hydrogen target.

We also wish to thank our scanning girls, Mme R. Blanc, Mme C. Bourgeois and Mlle V. Scarpetta, as well as our technicians Messrs. J. Berbiers, R. Maccaferri, O. Polgrossi and E. Stocco for their skillful assistance. The neutron counters were constructed at the Istituto di Fisica dell'Università di Bologna, and we would like to thank Messrs. W. Chiarini, G. Lelli, W. Lelli, F. Massera and G. Pacchioni for their hard work and their friendly collaboration.

* * *

Table 1

Theoretical predictions for $\Gamma_{\varphi \to e^+e^-}$	keV	Reference
Quark model	1.0	11
Current mixing model	2.2	7 and 8
Mass mixing model - 1	1.7	7 and 8
Mass mixing model - 2	1.2	7 and 8
DMO model	0.8	9
OS model	1.1	10
This experiment	2.1 ± 0.9	

REFERENCES

1) T. Massam, Th. Muller, M. Schneegans and A. Zichichi, Nuovo Cimento 39, 464 (1965).

2) T.C. Bacon, W.J. Fickinger, D.G. Hill, H.W.K. Hopkins, D.K. Robinson and E.O. Salant, Phys.Rev. 157, 1263 (1967).
M.A. Abolins, O.I. Dahl, J.S. Danburg, D. Davies, P. Hoch, J. Kirz, D.H. Miller and R. Rader, Proc.Int.Conf. on Elementary Particles, Heidelberg (1967) p. 509, and private communication.
O.I. Dahl, L.M. Hardy, R.I. Hess, J. Kirz and D.H. Miller, Phys.Rev. 163, 1377 (1967).

3) E. Ehlotzky and H. Mitter, Nuovo Cimento 55A, 181 (1968).

4) J.H. Boyd, A.R. Erwin, W.D. Walker and E. West, Phys.Rev. 166, 1458 (1968).

5) A.H. Rosenfeld, N. Barash-Schmidt, A. Barbaro-Galtieri, L.R. Price, P. Soding, C.G. Wohl, M. Roos and W.J. Willis, Rev.Mod.Phys. 40, 77 (1968).

6) R. Dashen and D. Sharp, Phys.Rev. 133B, 1585 (1964).

7) S. Coleman and H.J. Schnitzer, Phys.Rev. 134B, 863 (1964).

8) N.M. Kroll, T.D. Lee and B. Zumino, Phys.Rev. 157, 1376 (1967).

9) T. Das, V.S. Mathur and S. Okubo, Phys.Rev.Letters 19, 470 (1967).

10) R.J. Oakes and J.J. Sakurai, Phys.Rev.Letters 19, 1266 (1967).

11) R. van Royen and V.F. Weisskopf, Nuovo Cimento 50A, 617 (1967).
A. Dar and V.F. Weisskopf, Phys.Letters 26B, 670 (1968).

Figure captions

Fig. 1 : Schematic diagram of the experimental set-up.

Fig. 2 : Simplified block diagram of the electronic logic. (No details are shown of the M-counters, of the derivation of the signals from the sides 1 and 2 of the neutron detectors, nor of the veto-house logic.)

Fig. 3 : Kinematic curves in the $\vartheta - t_1$ plane: the dashed area represents the range accepted by the matrix "MASS" coincidence. During the run, this region was slightly modified to increase our efficiency.

Fig. 4 : Distribution of the distances between the two tracks of a "converted γ ray". The abscissa is the distance measured on the scanning table. Distances in real space are 6.2 times greater. The electron-positron events are similar to unresolved converted γ rays. The excess of events with zero distance shows that the e^+e^- events are genuine and are not due to materialized γ rays.

Fig. 5 : The mass distribution for those events with zero opening distance in Fig. 4. The mass used was the weighted mean mentioned in Section 1.

Fig. 6 : Photograph of a typical event: the two orthogonal views of each electron detector are shown. Notice that each detector is divided by the optics into two parts: left and right.

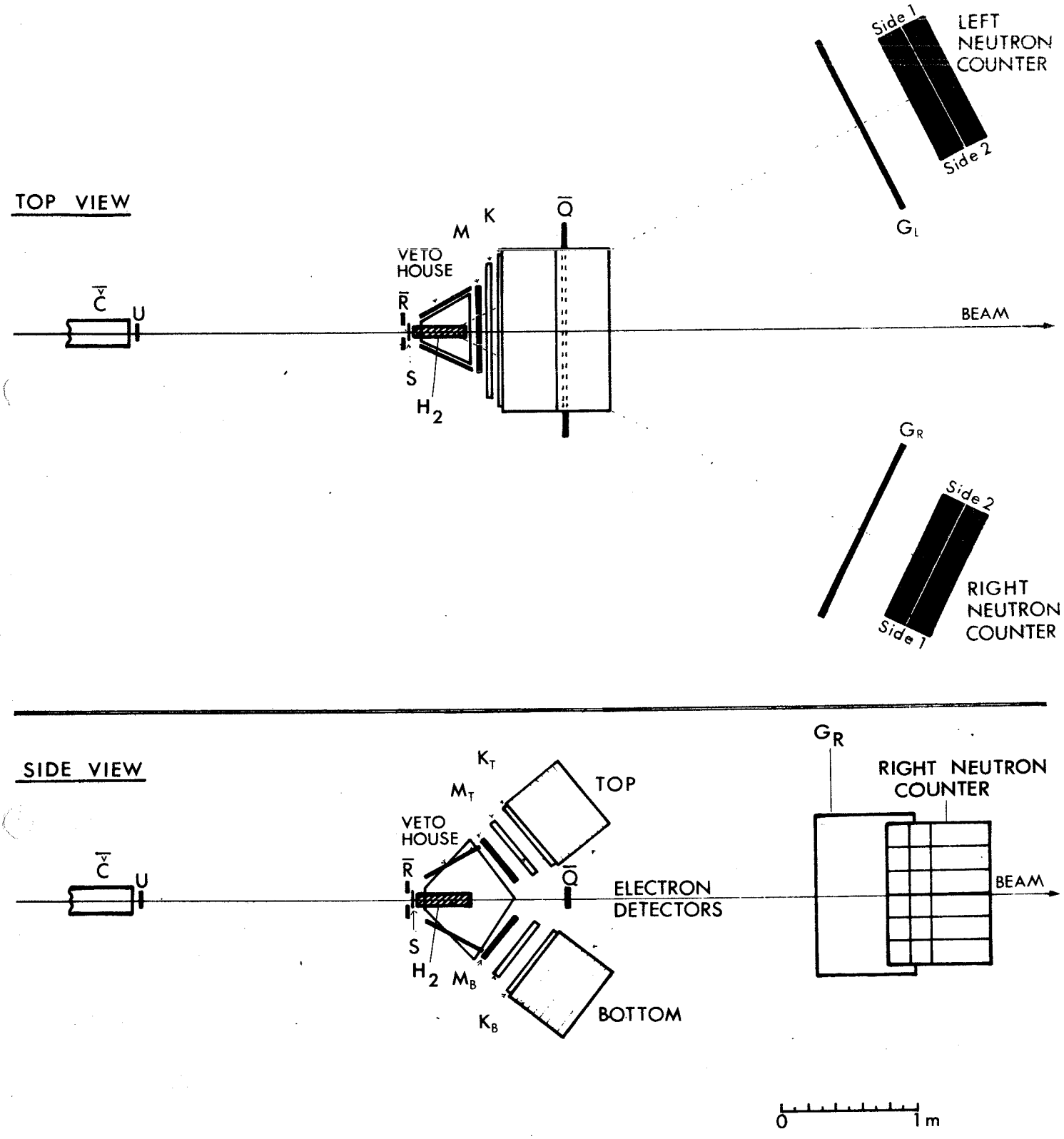

SCHEMATIC OF THE EXPERIMENTAL SET-UP

FIG. 1

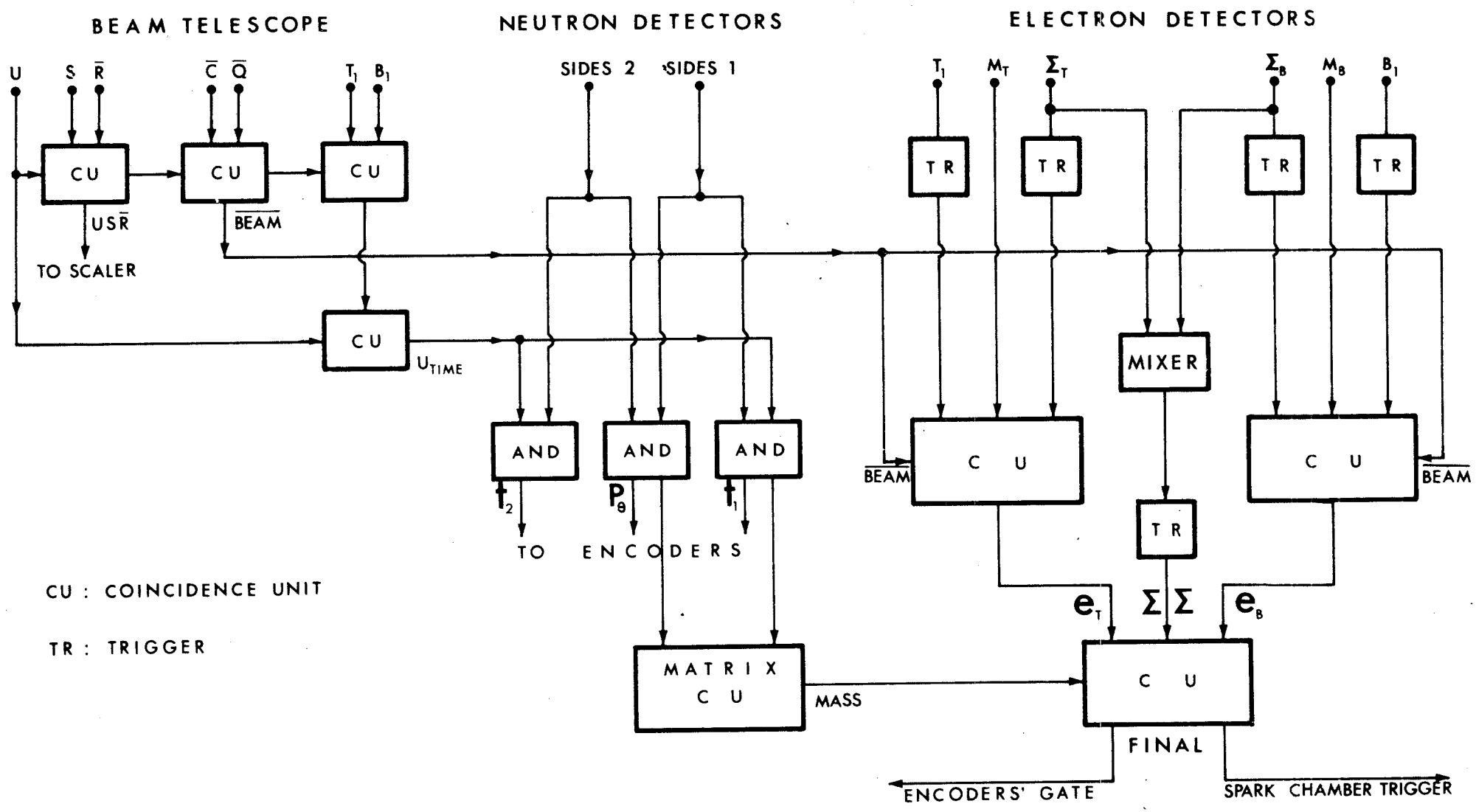

FIG. 2 – ELECTRONIC LOGIC

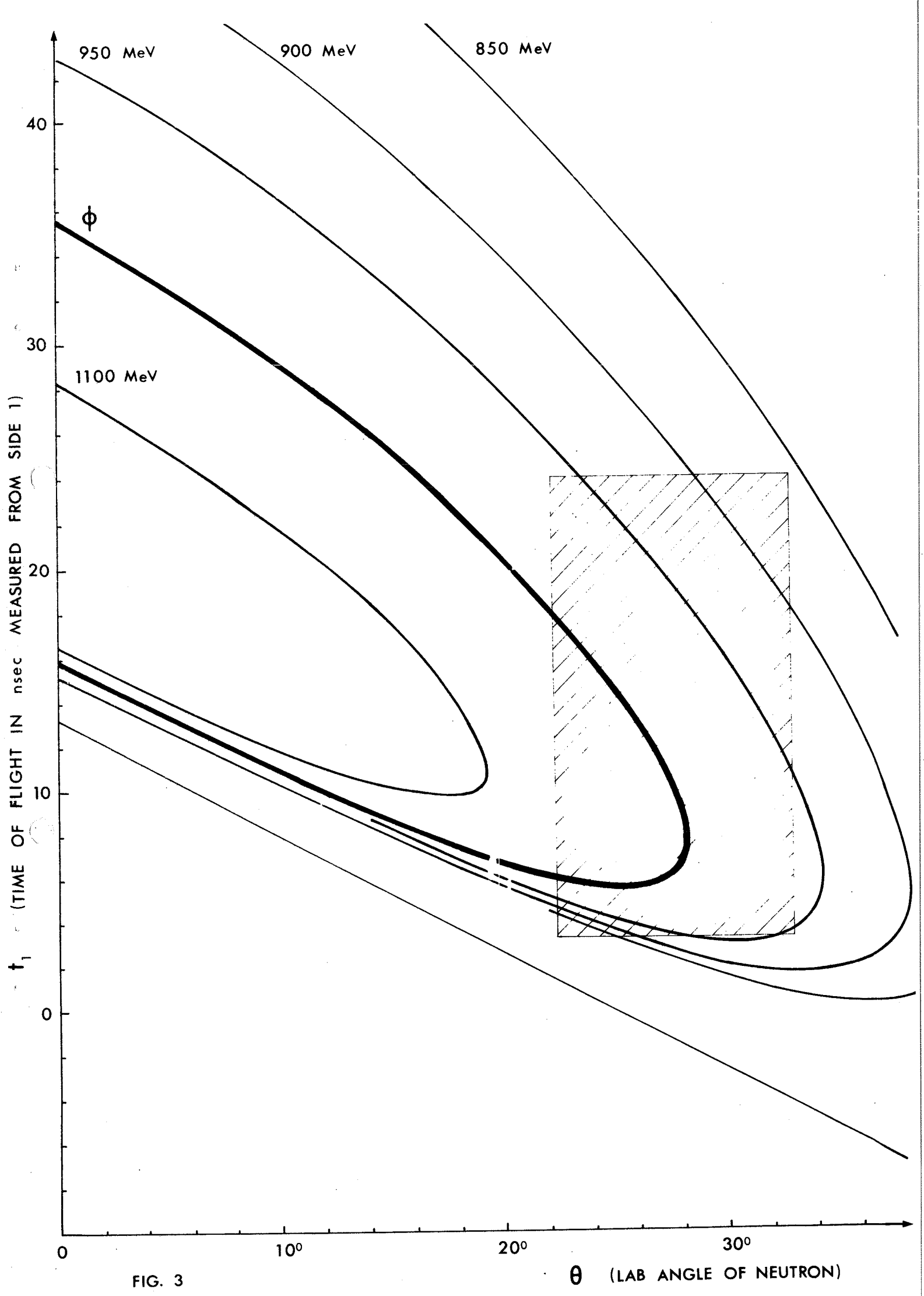
950 MeV
900 MeV
850 MeV
1100 MeV
φ
40
30
20
10
0
t_1 (TIME OF FLIGHT IN nsec MEASURED FROM SIDE 1)
0
10°
20°
30°
θ (LAB ANGLE OF NEUTRON)

FIG. 3

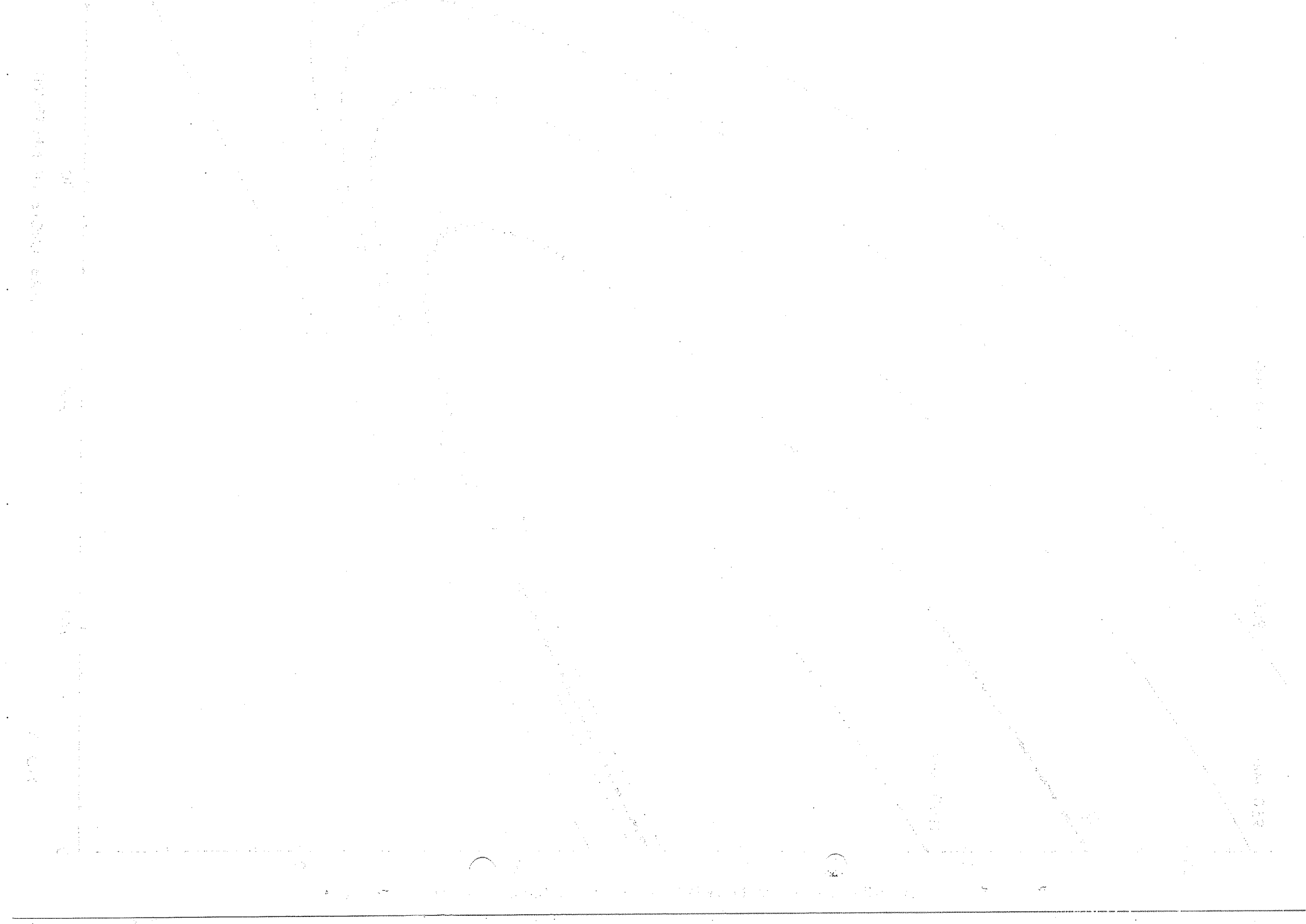

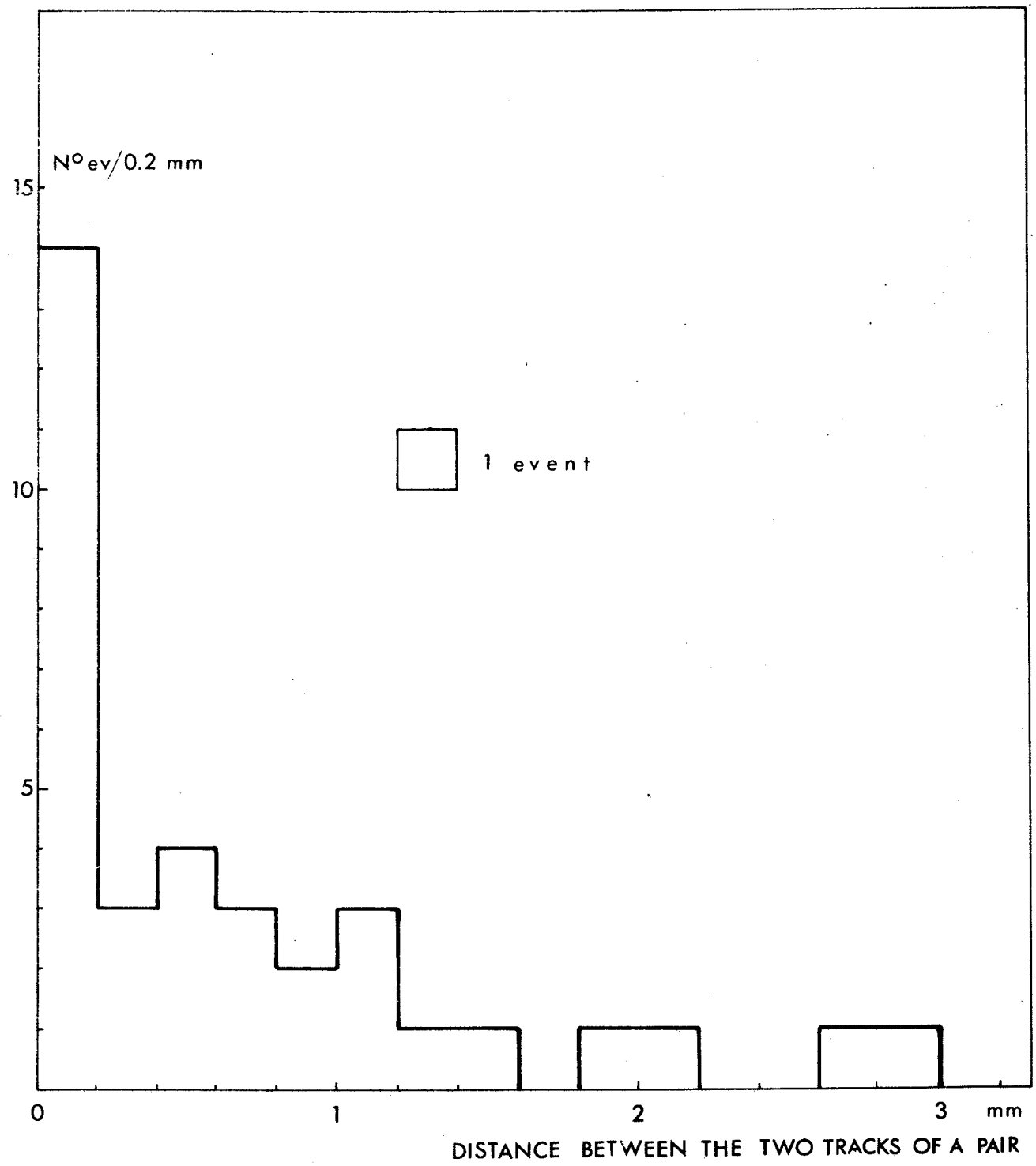
N°ev/0.2 mm
15
10
5
1 event
0
1
2
3
mm
DISTANCE BETWEEN THE TWO TRACKS OF A PAIR

FIG. 4

$\phi \rightarrow e^+ + e^-$

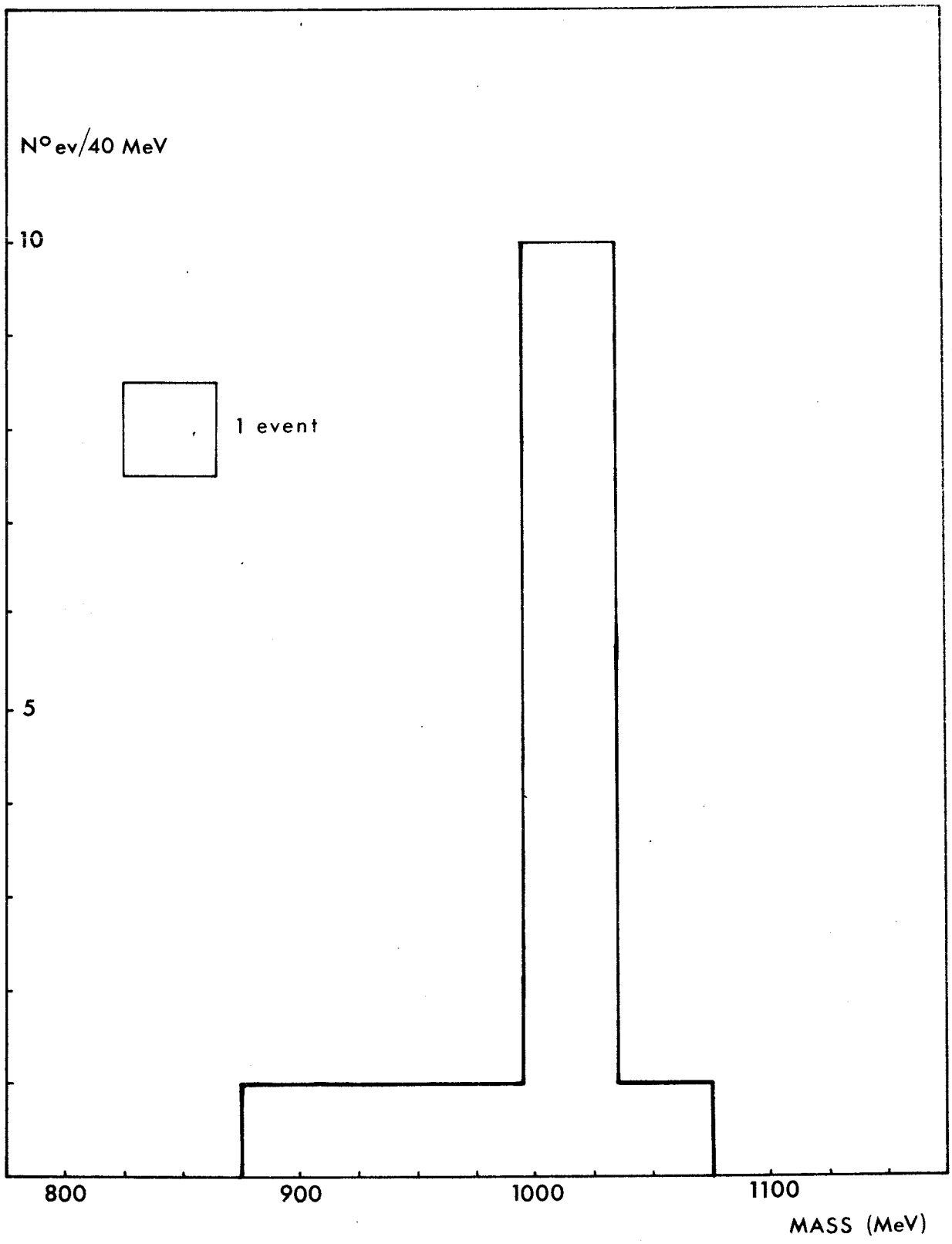

FIG. 5

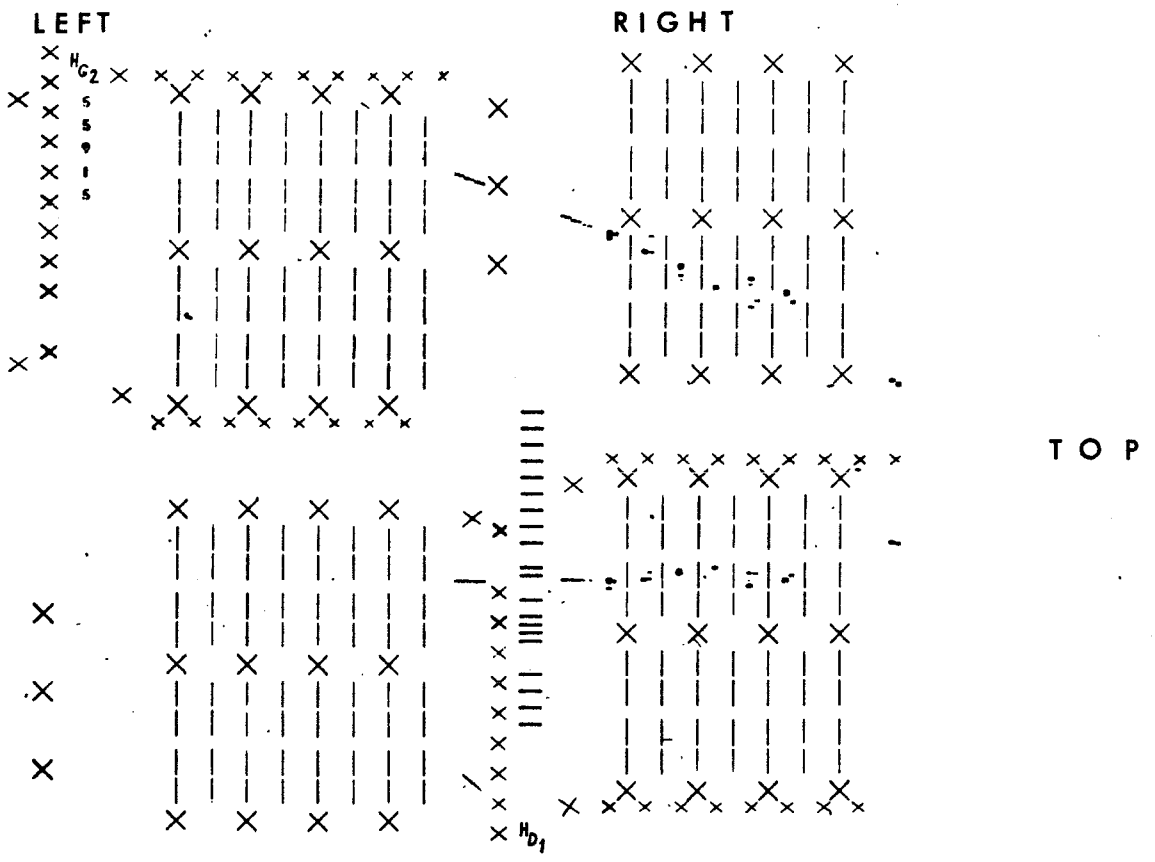

FIG. 6